



**HAL**  
open science

## Recent $^{210}\text{Pb}$ , $^{137}\text{Cs}$ and $^{241}\text{Am}$ accumulation in an ombrotrophic peatland from Amsterdam Island (Southern Indian Ocean)

Chuxian Li, Gaël Le Roux, Jeroen E. Sonke, Pieter van Beek, Marc Souhaut, Nathalie van Der Putten, François de Vleeschouwer

### ► To cite this version:

Chuxian Li, Gaël Le Roux, Jeroen E. Sonke, Pieter van Beek, Marc Souhaut, et al.. Recent  $^{210}\text{Pb}$ ,  $^{137}\text{Cs}$  and  $^{241}\text{Am}$  accumulation in an ombrotrophic peatland from Amsterdam Island (Southern Indian Ocean). *Journal of Environmental Radioactivity*, 2017, 175-176, pp.164-169. 10.1016/j.jenvrad.2017.05.004 . hal-03512169

**HAL Id: hal-03512169**

**<https://hal.science/hal-03512169>**

Submitted on 5 Jan 2022

**HAL** is a multi-disciplinary open access archive for the deposit and dissemination of scientific research documents, whether they are published or not. The documents may come from teaching and research institutions in France or abroad, or from public or private research centers.

L'archive ouverte pluridisciplinaire **HAL**, est destinée au dépôt et à la diffusion de documents scientifiques de niveau recherche, publiés ou non, émanant des établissements d'enseignement et de recherche français ou étrangers, des laboratoires publics ou privés.



## Open Archive Toulouse Archive Ouverte



OATAO is an open access repository that collects the work of Toulouse researchers and makes it freely available over the web where possible

This is an author's version published in: <http://oatao.univ-toulouse.fr/20952>

### Official URL:

<https://doi.org/10.1016/j.jenvrad.2017.05.004>

### To cite this version:

Li, Chuxian  and Le Roux, Gaël  and Sonke, Jeroen and van Beek, Pieter and Souhaut, Marc and Van der Putten, Nathalie and De Vleeschouwer, François  *Recent 210 Pb, 137 Cs and 241 Am accumulation in an ombrotrophic peatland from Amsterdam Island (Southern Indian Ocean)*. (2017) *Journal of Environmental Radioactivity*, 175-176. 164-169. ISSN 0265-931X

Any correspondence concerning this service should be sent to the repository administrator: [tech-oatao@listes-diff.inp-toulouse.fr](mailto:tech-oatao@listes-diff.inp-toulouse.fr)

# Recent $^{210}\text{Pb}$ , $^{137}\text{Cs}$ and $^{241}\text{Am}$ accumulation in an ombrotrophic peatland from Amsterdam Island (Southern Indian Ocean)

Chuxian Li <sup>a,\*</sup>, Gaël Le Roux <sup>a</sup>, Jeroen Sonke <sup>b</sup>, Pieter van Beek <sup>c</sup>, Marc Souhaut <sup>c</sup>, Nathalie Van der Putten <sup>d</sup>, François De Vleeschouwer <sup>a</sup>

<sup>a</sup> EcoLab, Université de Toulouse, CNRS, INPT, UPS, Tolosan, France

<sup>b</sup> Geoscience, Environment, Toulouse, Midi- Pyrénées Observatory, Toulouse, France

<sup>c</sup> LEGOS (CNRS/CNES/IRD/UPS), Midi- Pyrénées Observatory, Toulouse, France

<sup>d</sup> Department of Geology, Quaternary Sciences, Lund University, Lund, Sweden

## A B S T R A C T

Over the past 50 years,  $^{210}\text{Pb}$ ,  $^{137}\text{Cs}$  and  $^{241}\text{Am}$  have been abundantly used in reconstructing recent sediment and peat chronologies. The study of global aerosol climate interaction is also partially depending on our understanding of  $^{222}\text{Rn}$   $^{210}\text{Pb}$  cycling, as radionuclides are useful aerosol tracers. However, in comparison with the Northern Hemisphere, few data are available for these radionuclides in the Southern Hemisphere, especially in the South Indian Ocean. A peat core was collected in an ombrotrophic peatland from the remote Amsterdam Island (AMS) and was analyzed for  $^{210}\text{Pb}$ ,  $^{137}\text{Cs}$  and  $^{241}\text{Am}$  radionuclides using an underground ultra low background gamma spectrometer. The  $^{210}\text{Pb}$  Constant Rate of Supply (CRS) model of peat accumulations is validated by peaks of artificial radionuclides ( $^{137}\text{Cs}$  and  $^{241}\text{Am}$ ) that are related to nuclear weapon tests. We compared the AMS  $^{210}\text{Pb}$  data with an updated  $^{210}\text{Pb}$  deposition database. The  $^{210}\text{Pb}$  flux of  $98 \pm 6 \text{ Bq} \cdot \text{m}^{-2} \cdot \text{y}^{-1}$  derived from the AMS core agrees with data from Madagascar and South Africa. The elevated flux observed at such a remote location may result from the enhanced  $^{222}\text{Rn}$  activity and frequent rainfall in AMS. This enhanced  $^{222}\text{Rn}$  activity itself may be explained by continental air masses passing over southern Africa and/or Madagascar. The  $^{210}\text{Pb}$  flux at AMS is higher than those derived from cores collected in coastal areas in Argentina and Chile, which are areas dominated by marine westerly winds with low  $^{222}\text{Rn}$  activities. We report a  $^{137}\text{Cs}$  inventory at AMS of  $144 \pm 13 \text{ Bq} \cdot \text{m}^{-2}$  (corrected to 1969). Our data thus contribute to the under-represented data coverage in the mid latitudes of the Southern Hemisphere.

### Keywords:

Radionuclides

$^{210}\text{Pb}$

$^{137}\text{Cs}$

$^{241}\text{Am}$

Peat

Southern indian ocean

## 1. Introduction

Lead 210 ( $^{210}\text{Pb}$ ,  $T_{1/2} = 22.3$  years) dating is the most common method employed to estimate short term (from years to decades) chronologies in peat, estuarine, fluvial, and lacustrine environments (Le Roux and Marshall, 2011; Robbins and Edgington, 1975; Benoit and Rozan, 2001; Humphries et al., 2010).  $^{210}\text{Pb}$  originates from the decay of gaseous  $^{222}\text{Rn}$ , which escapes from the Earth's continental crust to the atmosphere (Graustein and Turekian, 1990).  $^{210}\text{Pb}$  adsorbs strongly to the surface of aerosols in the 0.1–0.5  $\mu\text{m}$  diameter size range as soon as it is produced in the air

(Knuth et al., 1983).  $^{210}\text{Pb}$  bearing aerosols are distributed globally by general atmospheric circulation and can be deposited on the Earth's surface mainly by precipitation, but also by dry fallout as well as convective updrafts (Knuth et al., 1983; Baskaran, 2011). The  $^{210}\text{Pb}$  deposited from the atmosphere is called “unsupported  $^{210}\text{Pb}$ ” or “excess  $^{210}\text{Pb}$ ” (denoted  $^{210}\text{Pb}_{\text{ex}}$ ), which should be distinguished from the  $^{210}\text{Pb}$  produced inside the matrix (e.g. lake sediment) and which is, named “supported  $^{210}\text{Pb}$ ” (Guevara et al., 2003).

The Constant Rate of Supply (CRS) model based on  $^{210}\text{Pb}_{\text{ex}}$  flux, which could be validated by nuclear fallout studies (e.g.  $^{137}\text{Cs}$ ,  $^{241}\text{Am}$ ), is by now widely used (e.g. Appleby et al., 2001, 2008). Another radionuclide that is widely used to derive ages is  $^{137}\text{Cs}$ . With a half life of 30.2 years,  $^{137}\text{Cs}$  is considered as one of the important radionuclides among those from nuclear emissions (e.g. atmospheric nuclear weapon tests in the 1950s 1970s with the peak in 1963 in the Northern Hemisphere and the fallout from the

\* Corresponding author. EcoLab (Laboratoire Ecologie Fonctionnelle et Environnement), ENSAT, Avenue de l'Agrobiopole, 31326 Castanet Tolosan, France.

E-mail address: chuxian.li@ensat.fr (C. Li).

Chernobyl accident in 1986), with respect to being a persistent tracer and an indicator of single event chronology (Aoyama et al., 2006; Rodway Dyer and Walling, 2010). In contrast,  $^{241}\text{Am}$  another artificial radionuclide is strictly related to nuclear bomb testing in remote areas.

Up to now, most studies about the inventory of sediment radionuclides and radiochronology have been conducted in the Northern Hemisphere. Limited work has been carried out in the Southern Hemisphere, especially in the Indian Ocean. The scarcity of studies conducted in the Southern Hemisphere is partly due to the lower fallout of  $^{210}\text{Pb}$  and  $^{137}\text{Cs}$ , fewer continental surfaces and fewer man made radionuclide emissions and fallout, which generally result in lower activities bordering on analytical detection limits (Owens and Walling, 1996; Bonotto and De Lima, 2006). In the Southern Hemisphere nuclear weapons fallout is about three times lower than that in the Northern Hemisphere. Consequently, the  $^{137}\text{Cs}$  fallout peak is usually more difficult to identify in cores due to the relatively high measurement uncertainties associated with the low  $^{137}\text{Cs}$  concentrations (Hancock et al., 2011). Southern Hemisphere investigations on  $^{210}\text{Pb}$  and  $^{137}\text{Cs}$  have been confined primarily to large land masses, such as South America (Sanders et al., 2006; Guevara et al., 2003; Cisternas et al., 2001), Australia and New Zealand (Pfitzner et al., 2004; Hancock et al., 2011) and South Africa and Madagascar (Humphries et al., 2010; Kading et al., 2009; Iva novitch and Harmon, 1992; Rabesiranana et al., 2016).

No studies on terrestrial sediment radionuclides and radio chronology exist for the Southern Indian Ocean, although the area is an important part of the global atmospheric and oceanic circulation patterns. Amsterdam Island (AMS,  $37^\circ\text{S}$ ) is located just north of the Subtropical Front (at approximately  $40^\circ\text{S}$ , Orsi et al., 1995), where cool, low salinity subpolar water submerges beneath warm, saline subtropical water (Prell et al., 1979). The island is located at the northern edge of both the Southern Westerly wind belt and the Antarctic Circumpolar Current.

The main objectives of this study were to investigate (1) to what extent observations in the Southern Indian Ocean could define Southern Hemisphere mid latitude  $^{210}\text{Pb}$ ,  $^{137}\text{Cs}$  and  $^{241}\text{Am}$  background conditions for the last 100 years and (2) how  $^{210}\text{Pb}$  levels are comparable between different matrices (e.g. wetland, sediment, glacier and atmospheric deposition) at different latitudes of the world, which could allow us to draw a new global sketch of  $^{210}\text{Pb}$  flux.

In this paper, for the very first time the inventories and fluxes of  $^{210}\text{Pb}$  and  $^{137}\text{Cs}$  together with a  $^{210}\text{Pb}$  based peat accumulation rate for AMS are reported. This island is located in Southern Indian Ocean at  $37^\circ\text{S}$  and at 3400 km from the nearest land mass. The atmospheric conditions at this location offer the possibility to potentially define  $^{210}\text{Pb}$  background concentrations, in a place with minimal perturbation from anthropogenic influences (Gaudichet et al., 1989; Angot et al., 2014). AMS is therefore an ideal site to investigate the background levels of  $^{210}\text{Pb}$ ,  $^{137}\text{Cs}$  and  $^{241}\text{Am}$  in the Southern Hemisphere, as well as to detect long range transport of anthropogenic radionuclides.

## 2. Materials and methods

### 2.1. Study area

AMS ( $37^\circ 50'\text{S}$ ,  $77^\circ 32'\text{E}$ ) is a small volcanic island with a surface of  $55\text{ km}^2$  and a maximum elevation of 881 m above sea level (a.s.l.). The center of the island is formed by a volcanic caldera in which an ombrotrophic peatland develops. The island is located at the northern edge of the westerly wind belt in the South Indian Ocean at a minimum distance of 3400 km and 5000 km upwind from the nearest land masses, respectively, Madagascar and South

Africa. The climate in AMS is mild oceanic, with frequent clouds (Angot et al., 2014). The annual precipitation is  $1124\text{ mm y}^{-1}$  based on 40 year annual average data from 1951 to 1990 (Meteo France data reported in Miller et al., 1993). The weather station is located at 29 m above sea level. However, although no record exists, the cloud accumulation at the top of the island makes the precipitation level much higher in the caldera than that recorded at the weather station. The orographic effect (Roe, 2005; Le Roux et al., 2008) would enhance precipitation and therefore,  $^{210}\text{Pb}$  bearing aerosols scavenging. Relatively higher volume of rainfall above 600 m a.s.l. also favors moss growth and peat accumulation in the caldera of AMS. The annual temperature is  $13.8^\circ\text{C}$  at the weather station, while the average annual humidity is 80% with little seasonal variations. Located in the middle of the Indian Ocean, AMS is also at the crossroads of African, Australian and Southern American dust trajectories (Li et al., 2008; Lamy et al., 2014).

### 2.2. Core sampling and sub sampling

One 5 m long peat sequence (AMS14 PB01A,  $37^\circ 50.742'\text{S}$ ,  $77^\circ 32.898'\text{E}$ ) was collected from the center of a raised bog at 738 m a.s.l. in December 2014 using a stainless steel Russian D corer of 10 cm internal diameter and 50 cm length (Belokopytov and Beresnevich, 1955; De Vleeschouwer et al., 2014; Vanneste et al., 2016) (Fig. 1). A second (AMS14 PB01B, 4.15 m length) and a third core (AMS14 PB01C, top 1 m length) at the same site were collected and stored as archives. All cores were photographed, described and wrapped in plastic film and PVC tubes before being shipped by boat to France in  $+4^\circ\text{C}$  fridges. Cores were frozen and subsequently sliced at roughly 1 cm resolution using a clean sub sampling procedure described in De Vleeschouwer et al. (2010). After being cleaned with MilliQ water and the edges removed (Givelet et al., 2004), the subsamples were dried using an ALPHA 1–4 LD plus freeze dryer. Prior to freeze drying, the dimensions of each sub sample were measured using a vernier caliper in order to i) obtain the volume for calculating the dry bulk density and ii) to estimate the cut loss between each slice by comparing the cumulative slices thickness and the total length of the core. In this paper, we focus on last 100–150 years of peat accumulation representing the top 12 cm of the master core.

### 2.3. Radiometric measurements

Fifteen freeze dried sample aliquots (approximately 0.3 g) were analyzed at the LAFARA underground laboratory located in Ferrières in the French Pyrénées (Van Beek et al., 2013). Prior to analysis, samples were sealed to prevent any  $^{222}\text{Rn}$  loss and stored for a period of 3 weeks to ensure radioactive equilibrium between  $^{226}\text{Ra}$ ,  $^{214}\text{Pb}$  and  $^{214}\text{Bi}$ . The  $^{210}\text{Pb}$ ,  $^{226}\text{Ra}$ ,  $^{137}\text{Cs}$  and  $^{241}\text{Am}$  activities were determined using a well type germanium detector that was protected from cosmic rays by 85 m of rock, thus yielding a very low background (Van Beek et al., 2013). The  $^{210}\text{Pb}$ ,  $^{137}\text{Cs}$  and  $^{241}\text{Am}$  were measured using the gamma lines at 46.5 keV, 661.7 keV and 59.5 keV, respectively. The  $^{226}\text{Ra}$  was determined using the 295 keV, 351.9 keV and 609.3 keV gamma emissions of its decay chain descendants ( $^{214}\text{Pb}$  and  $^{214}\text{Bi}$ ). Because of the very low activities present in the peat samples and because the volume of material to be analyzed was small, each sample was analyzed for at least four days. We used RGU1, RGTH1 and IAEA 375 standards provided by IAEA to calibrate the detector.

Excess  $^{210}\text{Pb}$  activities are calculated by correcting the total  $^{210}\text{Pb}$  for the  $^{210}\text{Pb}$  supported by  $^{226}\text{Ra}$ . Since the  $^{226}\text{Ra}$  activities were below the detection limit in the core, the  $^{210}\text{Pb}_{\text{ex}}$  activities are equivalent to the total  $^{210}\text{Pb}$  activities (Supplementary Table S1). In the following, we report  $^{210}\text{Pb}_{\text{ex}}$  activities. The detection limits

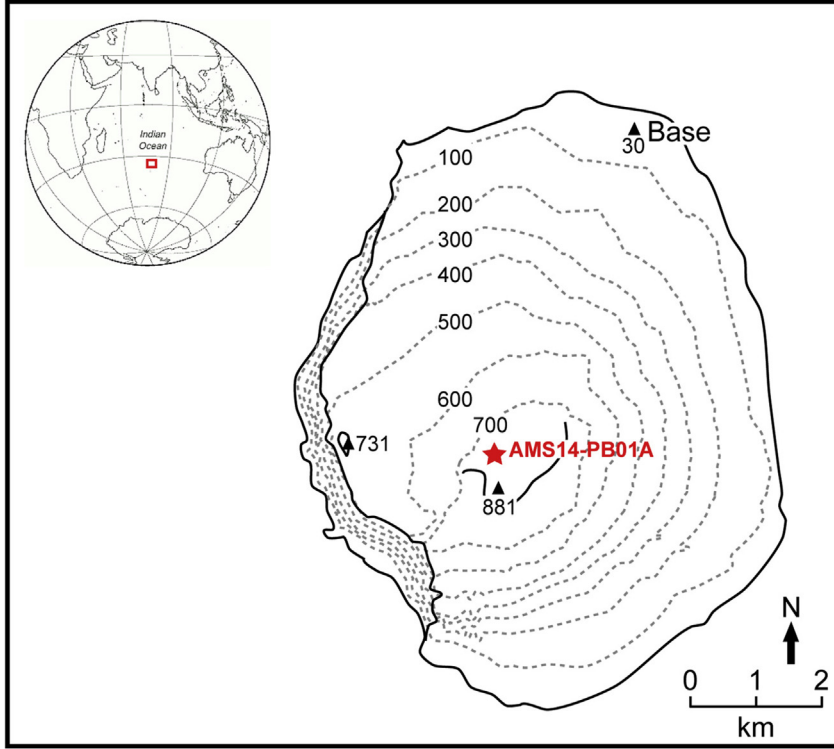


Fig. 1. Sampling site in Amsterdam Island.

achieved in this study (considering the low amount of material that was analyzed) were  $20 \text{ Bq}\cdot\text{kg}^{-1}$  for  $^{210}\text{Pb}$ ,  $0.4 \text{ Bq}\cdot\text{kg}^{-1}$  for  $^{137}\text{Cs}$  and  $0.6 \text{ Bq}\cdot\text{kg}^{-1}$  for  $^{241}\text{Am}$ .

#### 2.4. Calculating decays, fluxes and inventories

Atmospheric  $^{210}\text{Pb}$  fluxes  $\Phi$  ( $\text{Bq}\cdot\text{m}^{-2}\cdot\text{yr}^{-1}$ ) were calculated using:

$$\Phi = \lambda I_{210\text{Pb}} \quad (1)$$

where  $\lambda$  is the  $^{210}\text{Pb}$  day constant ( $0.03114 \text{ yr}^{-1}$ ,  $\lambda = \ln 2/T_{1/2}$ ) and  $I$  is the  $^{210}\text{Pb}_{\text{ex}}$  inventory ( $\text{Bq}\cdot\text{m}^{-2}$ ) in peat calculated from (Appleby, 1997):

$$I = \int_0^{\infty} \rho(x) \cdot C(x) \cdot dx \quad (2)$$

where  $\rho(x)$  ( $\text{g}\cdot\text{cm}^{-3}$ ) is the dry bulk density,  $dx$  is the soil thickness (cm) and  $C(x)$  is the excess  $^{210}\text{Pb}$  activity ( $\text{Bq}\cdot\text{kg}^{-1}$ ). (Sanchez Cabeza et al., 2007) The  $^{137}\text{Cs}$  inventory was also calculated using equation (2).

The formula for calculating  $^{137}\text{Cs}$  cumulative decay corrected fallout at year 1969 (maximum fallout, according to Aoyama et al., 2006) is shown below,

$$CD_{1969} = \sum_{\tau}^{1969} D_{\tau} e^{-\lambda(1969-\tau)} \quad (3)$$

$CD_{1969}$ : cumulative decay corrected fallout at year 1969 ( $\text{Bq}\cdot\text{m}^{-2}$ );  $\lambda$ : radioactive decay constant of  $^{137}\text{Cs}$  ( $0.023 \text{ yr}^{-1}$ ,  $\lambda = \ln 2/T_{1/2}$ );  $D_{\tau}$ : annual deposition of  $^{137}\text{Cs}$  at year  $\tau$  ( $\text{Bq}\cdot\text{m}^{-2}$ ).

### 3. Results and discussion

#### 3.1. Downcore distribution of $^{210}\text{Pb}$ , $^{137}\text{Cs}$ and $^{241}\text{Am}$ activities

Given that ombrotrophic peatlands are only depending on precipitation for their water balance,  $^{210}\text{Pb}$  flux is assumed to be exclusively of atmospheric origin at AMS. This is confirmed by the absence of supported  $^{210}\text{Pb}$  because no  $^{226}\text{Ra}$  was detected. Except for the first sample that contained living *Sphagnum* moss, the  $^{210}\text{Pb}_{\text{ex}}$  activities decrease with increasing depth down to approximately 12 cm. (Fig. 2 and Supplementary Table S1). As shown in Fig. 2, the activities of  $^{137}\text{Cs}$  and  $^{241}\text{Am}$  displayed peaks at the same depth (4.4–5.8 cm), with values of  $22 \pm 2 \text{ Bq}\cdot\text{kg}^{-1}$  and  $7 \pm 1 \text{ Bq}\cdot\text{kg}^{-1}$ , respectively, indicating that these peaks can be related to nuclear bomb testing (Spalding et al., 2005).

The total  $^{210}\text{Pb}_{\text{ex}}$  inventory was  $3160 \pm 200 \text{ Bq}\cdot\text{m}^{-2}$  with a corresponding  $^{210}\text{Pb}_{\text{ex}}$  flux of  $98 \pm 6 \text{ Bq}\cdot\text{m}^{-2}\cdot\text{y}^{-1}$ . According to equation (3), the corrected value for  $^{137}\text{Cs}$  inventory on AMS in 1969 was  $144 \pm 13 \text{ Bq}\cdot\text{m}^{-2}$ , which is two times lower than the modeled average inventory of  $580 \text{ Bq}\cdot\text{m}^{-2}$  (range from 150 to  $1430 \text{ Bq}\cdot\text{m}^{-2}$ ) at  $35^{\circ}\text{S}$  (Aoyama et al., 2006), but higher than the activity reported at  $45^{\circ}\text{S}$  in the same paper. Our observed  $^{137}\text{Cs}$  inventory for AMS is thus close to the lower limit of these estimates at  $35^{\circ}\text{S}$ .  $^{241}\text{Am}$  activity is relatively high showing potentially the immobility of this radioelement in the peat column compared to cesium. Despite this, the activity inventory ratio  $^{137}\text{Cs}/^{241}\text{Am}_{1969}$  1.2, derived from  $^{137}\text{Cs}$  and  $^{241}\text{Am}$  activities respectively, is on the same order of magnitude than what can be found in Antarctica and sub Antarctica islands (Pourchet et al., 2003; Roos et al., 1994).

#### 3.2. $^{210}\text{Pb}$ chronology

Well dated peat profiles are valuable archives of past environmental changes. The Constant Rate of Supply (CRS) model (Appleby,

1997; Binford, 1990) was applied to  $^{210}\text{Pb}$  inventories calculated from the  $^{210}\text{Pb}_{\text{ex}}$  data to generate ages. The peat core presented here spans a period of about 157 years, indicating a peat accumulation rate of about  $0.75 \text{ mm yr}^{-1}$ .

Oldfield et al. (1995) suggested that  $^{210}\text{Pb}$  measurements alone cannot result in an accurate chronology of peat accumulation. However, when constrained by  $^{241}\text{Am}$  and  $^{137}\text{Cs}$  activity profiles in the upper part of a sequence,  $^{210}\text{Pb}$  can provide good chronologies of peat accumulation. The  $^{210}\text{Pb}_{\text{ex}}$  dates from the peat profile in AMS calculated using the CRS model were independently validated by  $^{137}\text{Cs}$  and  $^{241}\text{Am}$  that displayed highest activities between 1960 and 1981 (Fig. 3), corresponding to the period of nuclear weapon tests (i.e. in the 1960s). Moreover the detection of  $^{241}\text{Am}$  excludes the possibility that  $^{137}\text{Cs}$  post depositional mobility processes would have shifted the  $^{137}\text{Cs}$  activity maximum (Schettler et al., 2006 Part B).

### 3.3. $^{210}\text{Pb}$ flux in AMS compared with global $^{210}\text{Pb}$ depositional flux

We updated the database from Turekian et al. (1977) and Preiss (1997) by compiling 47 new entries from the last 20 years. Global estimates of  $^{210}\text{Pb}$  flux from the literature, integrated over  $30^\circ$  latitudinal belts within different matrices, are shown in Fig. 4 and Supplementary Table S2. Only terrestrial data, i.e. from wetlands (peatlands, salt marshes and swamps), sediments (lakes, estuarine and soil profiles), glaciers (ice core and firn) as well as atmospheric deposition (snow, precipitation plus dry fallout) are included.

Globally, the  $^{210}\text{Pb}$  flux measured in wetland sequences show smaller uncertainties compared to fluxes measured from atmospheric deposition and sediment sequences (Fig. 4). The dominant  $^{210}\text{Pb}$  input to wetlands is through the atmosphere in contrast to lake basins and the data are integrated over several years (1 cm layer represents a period of more than 10 years). The relatively larger uncertainty observed in atmospheric deposition could be explained by short term measurements (i.e. annual) that can enhance different tropospheric contributions. Many factors (e.g., adjoining drainage areas) could alter the  $^{210}\text{Pb}$  flux in sediment sequences.

In general, the  $^{210}\text{Pb}$  flux is lower at high latitudes ( $>60^\circ$  latitude) (Fig. 4), especially when measured in glaciers and atmospheric deposition, where the low density of land masses results in lower  $^{222}\text{Rn}$  emissions. According to the existing data, the  $^{210}\text{Pb}$  fluxes measured in sediments are higher than those measured in the other three categories in the Northern Hemisphere, while in the Southern Hemisphere the values detected in wetlands are the

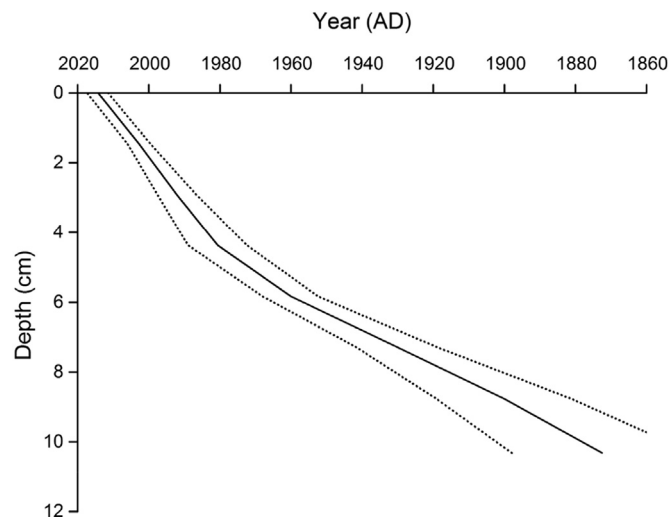


Fig. 3.  $^{210}\text{Pb}_{\text{ex}}$  inferred chronology based on CRS model.

highest (except between  $60$  and  $90^\circ\text{S}$  where no measurement exists). The  $^{210}\text{Pb}$  fluxes from atmospheric deposition are similar to those from wetlands in the Northern Hemisphere (Fig. 4). Wetlands are found to be the appropriate archives for a good estimation of atmospheric flux, due to the absence of in wash of sediments, and the low energy budget (absence of streams)(Preiss et al., 1996). However in the Southern Hemisphere,  $^{210}\text{Pb}$  flux from wetlands and atmospheric deposition are not similar, which might be partially due to the scarcity of data (only 7 for wetlands) resulting in a non representative dataset. Compared to the Northern Hemisphere, fewer data are available for the Southern Hemisphere, and thus more effort should be made in the future to fill this gap.

In the peat core from AMS, the  $^{210}\text{Pb}$  flux was  $98 \pm 6 \text{ Bq}\cdot\text{m}^{-2}\cdot\text{y}^{-1}$ , which is higher than most values reported at around  $40^\circ\text{S}$ . For example, Baskaran (2011) found an average  $^{210}\text{Pb}$  flux of  $61 \pm 2 \text{ Bq}\cdot\text{m}^{-2}\cdot\text{y}^{-1}$  between  $30$  and  $40^\circ\text{S}$  and  $42 \text{ Bq}\cdot\text{m}^{-2}\cdot\text{y}^{-1}$  between  $40$  and  $50^\circ\text{S}$  based on terrestrial or marine settings. Guelle et al. (1998) used three kinds of wet scavenging schemes to simulate the  $^{210}\text{Pb}$  distribution and found a flux of  $28\text{--}34 \text{ Bq}\cdot\text{m}^{-2}\cdot\text{y}^{-1}$  between  $30$  and  $60^\circ\text{S}$ . The  $^{210}\text{Pb}$  atmospheric

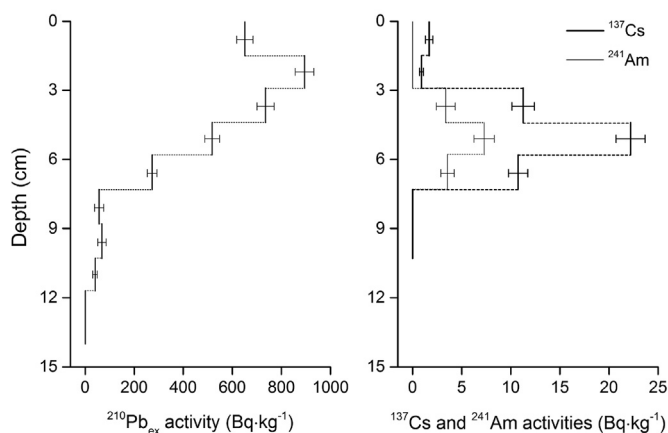


Fig. 2. Vertical profiles of  $^{210}\text{Pb}_{\text{ex}}$ ,  $^{137}\text{Cs}$  and  $^{241}\text{Am}$  activities in the peat core collected in Amsterdam Island.

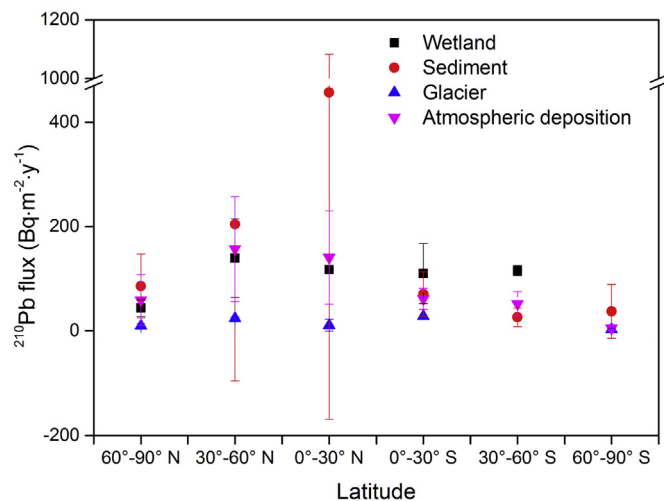


Fig. 4. Global atmospheric depositional fluxes of  $^{210}\text{Pb}$  among different matrices at different latitude. (Data assembled from Supplementary Table S2).

deposition in Tasmania is  $41.5 \text{ Bq} \cdot \text{m}^{-2} \cdot \text{y}^{-1}$  ( $42.5^\circ\text{S}$ ,  $147.5^\circ\text{E}$ ) (Preiss, 1997). Rosen (1957) found a much lower value ( $1.24 \text{ Bq} \cdot \text{m}^{-2} \cdot \text{y}^{-1}$ ) in Wellington ( $41^\circ 17'\text{S}$ ), New Zealand based on the calculation of the  $^{222}\text{Rn}$  flux. The estimated unsupported  $^{210}\text{Pb}$  fluxes values from the global model made by Turekian et al. (1977) and El Daoushy (1988) were  $\leq 74$  (in terrestrial settings) and  $58.4 \text{ Bq} \cdot \text{m}^{-2} \cdot \text{y}^{-1}$ , respectively. Unsupported  $^{210}\text{Pb}$  flux from lake sediments in Northern Patagonia (from  $40^\circ 30'\text{S}$  to  $41^\circ 10'\text{S}$ ) showed very low values, ranging between 4 and  $48 \text{ Bq} \cdot \text{m}^{-2} \cdot \text{y}^{-1}$  (Guevara et al., 2003). The average  $^{210}\text{Pb}$  flux from lake sediment in central Chile ( $36^\circ 51'\text{S}$ ,  $73^\circ 05'\text{W}$ ) was  $23.6 \text{ Bq} \cdot \text{m}^{-2} \cdot \text{y}^{-1}$  (Cisternas et al., 2001). However, when compared with a soil profile from Madagascar, we find almost the same value ( $95.8 \text{ Bq} \cdot \text{m}^{-2} \cdot \text{y}^{-1}$ , Rabesiranana et al., 2016) as in AMS. Our value is also quite similar to other values obtained from swamps or salt marshes found in South Africa ( $139 \pm 37 \text{ Bq} \cdot \text{m}^{-2} \cdot \text{y}^{-1}$ , n = 4, Humphries et al., 2010; Kading et al., 2009; Ivanovich and Harmon, 1992). The  $^{210}\text{Pb}$  flux in AMS is lower than some measurements conducted in wetlands between  $30^\circ$  and  $60^\circ\text{N}$ , e.g., Romania (between 133 and  $277 \text{ Bq} \cdot \text{m}^{-2} \cdot \text{y}^{-1}$ , Begy et al., 2016), China (254 and  $421 \text{ Bq} \cdot \text{m}^{-2} \cdot \text{y}^{-1}$ , Bao et al., 2010).

Depositional flux of  $^{210}\text{Pb}$  at any given site depends on the local  $^{222}\text{Rn}$  emanation rates and the relative proportion of maritime and continental air masses along with the differences in the amount and frequency of precipitation (Baskaran, 2011). The highly variable  $^{210}\text{Pb}$  depositional fluxes give insight into the sources and sinks of aerosols. The study sites in Argentina and Chile (Cisternas et al., 2001; Guevara et al., 2003), showing much lower  $^{210}\text{Pb}$  fluxes, are located at the coast near the Pacific Ocean, and are influenced by westerly winds bringing oceanic air masses. The contribution of sea salt for  $^{210}\text{Pb}$  from oceanic  $^{222}\text{Rn}$  is negligible. Global  $^{222}\text{Rn}$  flux from continents is estimated to be around  $1300\text{--}1800 \text{ Bq} \cdot \text{m}^{-2} \cdot \text{d}^{-1}$ , which is around 2 orders of magnitude higher than that from the oceans (Samuelsson et al., 1986; Nazaroff, 1992). The  $^{210}\text{Pb}$  flux at AMS is relatively high (discussed above). Despite the remoteness of the island, Angot et al. (2014) found that air masses passing over the southern African continent and/or Madagascar could enhance  $^{222}\text{Rn}$  activity in AMS based on the study of back trajectory. Continental air masses originating from South Africa and/or Madagascar are enriched in  $^{210}\text{Pb}$  that is then scavenged to clouds over the Indian Ocean. The regular orographic heavy rainfalls in the caldera at the top of AMS promote the deposition of  $^{210}\text{Pb}$  from the South Africa and/or Madagascar air masses into the peatland, resulting in a  $^{210}\text{Pb}$  flux on the island similar to those in South Africa and Madagascar.

#### 4. Conclusion

For the very first time, radionuclide ( $^{210}\text{Pb}$ ,  $^{137}\text{Cs}$ ,  $^{241}\text{Am}$ ) measurements conducted in a peat core taken from an ombrotrophic peatland on AMS are presented. The chronology based on  $^{210}\text{Pb}$  using a CRS model is consistent with other chronomarkers ( $^{137}\text{Cs}$  and  $^{241}\text{Am}$ ), which allows the reconstruction of a peat mass accumulation rate of  $0.75 \text{ mm yr}^{-1}$  for a period of 157 years. The  $^{210}\text{Pb}$  flux of  $98 \pm 6 \text{ Bq} \cdot \text{m}^{-2} \cdot \text{y}^{-1}$  measured in the peat core is relatively high compared to many observations at around  $40^\circ\text{S}$ . This pattern might be explained by the fact that, most studies conducted in the mid latitudes in Southern Hemisphere are located on the west side of the continents, close to the coast, and are highly influenced by westerly winds bringing air masses with low  $^{222}\text{Rn}$  activities. However, the  $^{210}\text{Pb}$  flux at AMS is comparable to the ones in South Africa and Madagascar. This may be explained by the continental air mass enriched in  $^{222}\text{Rn}$  originating from South Africa and/or Madagascar influencing AMS together with the frequent and heavy rainfalls at the top of the island which would enhance deposition. The  $^{137}\text{Cs}$  inventory was  $144 \pm 13 \text{ Bq} \cdot \text{m}^{-2}$  (corrected to 1969). Since

no terrestrial studies were conducted in the south Indian Ocean, the data reported here from AMS ( $^{210}\text{Pb}$ ,  $^{137}\text{Cs}$  and  $^{241}\text{Am}$ ) are of value for the global database.

#### Acknowledgements

We are grateful to Svante Björck, Bart Klink and Elisabeth Michel for their help during fieldwork. These results would never have been obtained if we had not had the incredible support of the Mission 66 of Amsterdam Island. Very special thanks to Alain Quivoron and Hubert Launay. The field expedition of this project was supported by IPEV project 1066 PARAD to FDV. We are very grateful to Nina Marchand (IPEV) for the incredible logistical support and Cédric Marteau for making the sampling possible in the protected areas of the TAAF Nature Reserve. Chuxian Li's PhD is supported by a scholarship from the Chinese Scholarship Council (No. 201506990002). We are grateful to EDF (Electricité De France) for allowing us to run our germanium detectors in the tunnel of Ferrières. We thank the European Union and Région Occitanie Pyrénées Méditerranée for supporting the LAFARA underground laboratory through a FEDER funding (SELECT project). We finally thank the 4 anonymous reviewers for their useful comments that greatly improved the quality of this manuscript.

#### Appendix A. Supplementary data

Supplementary data related to this article can be found at <http://dx.doi.org/10.1016/j.jenvrad.2017.05.004>.

#### References

- Angot, H., Barret, M., Magand, O., Ramonet, M., Dommergue, A., 2014. A 2-year record of atmospheric mercury species at a background Southern Hemisphere station on Amsterdam Island. *Atmos. Chem. Phys.* 14 (20), 11461–11473.
- Aoyama, M., Hirose, K., Igarashi, Y., 2006. Re-construction and updating our understanding on the global weapons tests 137 Cs fallout. *J. Environ. Monit.* 8 (4), 431–438.
- Appleby, P., 1997. In Dating recent sediments by  $^{210}\text{Pb}$ : problems and solutions. Helsinki. In: Proc. 2nd NKS/EKO-1 Seminar.
- Appleby, P., Birks, H.H., Flower, R.J., Rose, N., Peglar, S.M., Ramdani, M., Kraiem, M.M., Fathi, A.A., 2001. Radiometrically determined dates and sedimentation rates for recent sediments in nine North African wetland lakes (the CASSARINA Project). *Aquat. Ecol.* 35 (3–4), 347–367 (a).
- Appleby, P., 2008. Three decades of dating recent sediments by fallout radionuclides: a review. *Holocene* 18 (1), 83–93 (b).
- Bao, K., Xia, W., Lu, X., Wang, G., 2010. Recent atmospheric lead deposition recorded in an ombrotrophic peat bog of Great Hinggan Mountains, Northeast China, from  $^{210}\text{Pb}$  and  $^{137}\text{Cs}$  dating. *J. Environ. Radioact.* 101 (9), 773–779.
- Baskaran, M., 2011. Po-210 and Pb-210 as atmospheric tracers and global atmospheric Pb-210 fallout: a review. *J. Environ. Radioact.* 102 (5), 500–513.
- Begy, R.C., Kovacs, T., Veres, D., Simon, H., 2016. Atmospheric flux, transport and mass balance of  $^{210}\text{Pb}$  and  $^{137}\text{Cs}$  radiotracers in different regions of Romania. *Appl. Radiat. Isotopes* 111, 31–39.
- Belokopytov, I., Beresnevich, V., 1955. Giktorf's peat borers. *Torfyanaia Promyshlennost* 8, 9–10.
- Benoit, G., Rozan, T.F., 2001.  $^{210}\text{Pb}$  and  $^{137}\text{Cs}$  dating methods in lakes: a retrospective study. *J. Paleolimnol.* 25 (4), 455–465.
- Binford, M.W., 1990. Calculation and uncertainty analysis of  $^{210}\text{Pb}$  dates for PIRLA project lake sediment cores. *J. Paleolimnol.* 3 (3), 253–267.
- Bonotto, D.M., De Lima, J., 2006.  $^{210}\text{Pb}$ -derived chronology in sediment cores evidencing the anthropogenic occupation history at Corumbataí River basin, Brazil. *Environ. Geol.* 50 (4), 595–611.
- Cisternas, M., Aranedo, A., Martínez, P., Pérez, S., 2001. Effects of historical land use on sediment yield from a lacustrine watershed in central Chile. *Earth Surf. Process. Landforms* 26 (1), 63–76.
- De Vleeschouwer, F., Chambers, F.M., Swindles, G.T., 2010. Coring and sub-sampling of peatlands for palaeoenvironmental research. *Mires Peat* 7.
- De Vleeschouwer, F., Vanneste, H., Mauquoy, D., Piotrowska, N., Torrejón, F., Roland, T., Stein, A., Le Roux, G., 2014. Emissions from pre-Hispanic metallurgy in the South American atmosphere. *PLoS One* 9 (10), e111315.
- El-Daoushy, F., 1988. A summary on the lead-210 cycle in nature and related applications in Scandinavia. *Environ. Int.* 14 (4), 305–319.
- Gaudichet, A., Lefevre, R., Gaudry, A., Ardouin, B., Lambert, G., Miller, J., 1989. Mineralogical composition of aerosols at Amsterdam island. *Tellus B* 41 (3), 344–352.

- Givelet, N., Le Roux, G., Cheburkin, A., Chen, B., Frank, J., Goodsite, M.E., Kempter, H., Krachler, M., Noernberg, T., Rausch, N., 2004. Suggested protocol for collecting, handling and preparing peat cores and peat samples for physical, chemical, mineralogical and isotopic analyses. *J. Environ. Monit.* 6 (5), 481–492.
- Graustein, W.C., Turekian, K.K., 1990. Radon fluxes from soils to the atmosphere measured by  $^{210}\text{Pb}$   $^{226}\text{Ra}$  disequilibrium in soils. *Geophys. Res. Lett.* 17 (6), 841–844.
- Guelle, W., Balkanski, Y., Dibb, J.E., Schulz, M., Dulac, F., 1998. Wet deposition in a global size-dependent aerosol transport model: 2. Influence of the scavenging scheme on  $^{210}\text{Pb}$  vertical profiles, surface concentrations, and deposition. *J. Geophys. Res. Atmos.* 103 (D22), 28875–28891.
- Guevara, S.R., Rizzo, A., Sánchez, R., Arribère, M., 2003.  $^{210}\text{Pb}$  fluxes in sediment layers sampled from Northern Patagonia lakes. *J. Radioanalytical Nucl. Chem.* 258 (3), 583–595.
- Hancock, G., Leslie, C., Everett, S., Tims, S., Brunskill, G., Haese, R., 2011. Plutonium as a chronometer in Australian and New Zealand sediments: a comparison with  $^{137}\text{Cs}$ . *J. Environ. Radioact.* 102 (10), 919–929.
- Humphries, M.S., Kindness, A., Ellery, W.N., Hughes, J.C., Benitez-Nelson, C.R., 2010.  $^{137}\text{Cs}$  and  $^{210}\text{Pb}$  derived sediment accumulation rates and their role in the long-term development of the Mkuze River floodplain, South Africa. *Geomorphology* 119 (1), 88–96.
- Ivanovich, M., Harmon, R.S., 1992. Uranium-series Disequilibrium: Applications to Earth, Marine, and Environmental Sciences, vol. 2.
- Kading, T., Mason, R., Leaner, J., 2009. Mercury contamination history of an estuarine floodplain reconstructed from a  $^{210}\text{Pb}$ -dated sediment core (Berg River, South Africa). *Mar. Pollut. Bull.* 59 (4), 116–122.
- Knuth, R.H., et al., 1983. "Size distribution of atmospheric Pb and  $^{210}\text{Pb}$  in rural New Jersey: implications for wet and dry deposition." Precipitation scavenging, dry deposition, and resuspension. In: Proceedings, vol. 2.
- Lamy, F., Gersonde, R., Winckler, G., Esper, O., Jaeschke, A., Kuhn, G., Ullermann, J., Martínez-García, A., Lambert, F., Kilian, R., 2014. Increased dust deposition in the Pacific Southern Ocean during glacial periods. *Science* 343 (6169), 403–407.
- Le Roux, G., et al., 2008. Aerosol deposition and origin in French mountains estimated with soil inventories of  $^{210}\text{Pb}$  and artificial radionuclides. *Atmos. Environ.* 42.7, 1517–1524.
- Le Roux, G., Marshall, W.A., 2011. Constructing recent peat accumulation chronologies using atmospheric fall-out radionuclides. *Mires Peat* 7.1, e14.
- Li, F., Ginoux, P., Ramaswamy, V., 2008. Distribution, transport, and deposition of mineral dust in the Southern Ocean and Antarctica: contribution of major sources. *J. Geophys. Res. Atmos.* 113 (D10).
- Miller, J.M., et al., 1993. A 10-year trajectory flow climatology for Amsterdam island, 1980–1989. *Atmos. Environ. Part A. Gen. topics* 27 (12), 1909–1916.
- Nazaroff, W.W., 1992. Radon transport from soil to air. *Rev. Geophys.* 30 (2), 137–160.
- Oldfield, F., Richardson, N., Appleby, P., 1995. Radiometric dating ( $^{210}\text{Pb}$ ,  $^{137}\text{Cs}$ ,  $^{241}\text{Am}$ ) of recent ombrotrophic peat accumulation and evidence for changes in mass balance. *Holocene* 5 (2), 141–148.
- Orsi, Alejandro H., Whitworth, Thomas, Nowlin, Worth D., 1995. On the meridional extent and fronts of the Antarctic Circumpolar Current. *Deep Sea Res. Part I Oceanogr. Res. Pap.* 42.5, 641–673.
- Owens, P.N., Walling, D.E., 1996. Spatial variability of caesium-137 inventories at reference sites: an example from two contrasting sites in England and Zimbabwe. *Appl. Radiat. isotopes* 47 (7), 699–707.
- Pfiftner, J., Brunskill, G., Zagorskis, I., 2004.  $^{137}\text{Cs}$  and excess  $^{210}\text{Pb}$  deposition patterns in estuarine and marine sediment in the central region of the Great Barrier Reef Lagoon, north-eastern Australia. *J. Environ. Radioact.* 76 (1), 81–102.
- Pourchet, M., et al., 2003. Radionuclides deposition over Antarctica. *J. Environ. Radioact.* 68.2, 137–158.
- Preiss, N., 1997. Etude du  $^{210}\text{Pb}$  d'origine atmosphérique dans l'air, la neige, les sols et les sédiments: Mesures, inventaires et interprétation à l'échelle globale.
- Preiss, N., Mélières, M.A., Pourchet, M., 1996. A compilation of data on lead  $^{210}\text{Pb}$  concentration in surface air and fluxes at the air-surface and water-sediment interfaces. *J. Geophys. Res. Atmos.* 101 (D22), 28847–28862.
- Prell, Warren L., William, H. Hutson, Williams, Douglas F., 1979. The subtropical convergence and late Quaternary circulation in the southern Indian Ocean. *Mar. Micropaleontol.* 4, 225–234.
- Rabesiranana, N., Rasolonirina, M., Solonjara, A., Ravoson, H., Andriambololona, R., Mabit, L., 2016. Assessment of soil redistribution rates by  $^{137}\text{Cs}$  and  $^{210}\text{Pb}$  ex in a typical Malagasy agricultural field. *J. Environ. Radioact.* 152, 112–118.
- Robbins, J.A., Edgington, D., 1975. Determination of recent sedimentation rates in Lake Michigan using  $^{210}\text{Pb}$  and  $^{137}\text{Cs}$ . *Geochimica Cosmochimica Acta* 39 (3), 285–304.
- Rodway-Dyer, S., Walling, D., 2010. The use of  $^{137}\text{Cs}$  to establish longer-term soil erosion rates on footpaths in the UK. *J. Environ. Manag.* 91 (10), 1952–1962.
- Roe, Gerard H., 2005. Orographic precipitation. *Annu. Rev. Earth Planet. Sci.* 33, 645–671.
- Roos, P., et al., 1994. Deposition of  $^{210}\text{Pb}$ ,  $^{137}\text{Cs}$ ,  $^{239}+^{240}\text{Pu}$ ,  $^{238}\text{Pu}$ , and  $^{241}\text{Am}$  in the antarctic peninsula area. *J. Environ. Radioact.* 24.3, 235–251.
- Rosen, R., 1957. Note on some observations of radon and thoron exhalation from the ground. *NZJ Sci. Technol.* 38, 644–654.
- Samuelsson, C., Hallstadius, L., Persson, B., Hedvall, R., Holm, E., Forkman, B., 1986.  $^{222}\text{Rn}$  and  $^{210}\text{Pb}$  in the Arctic summer air. *J. Environ. Radioact.* 3 (1), 35–54.
- Sanchez-Cabeza, J.-A., Garcia-Talavera, M., Costa, E., Pena, V., Garcia-Orellana, J., Masqué, P., Nalda, C., 2007. Regional calibration of erosion radiotracers ( $^{210}\text{Pb}$  and  $^{137}\text{Cs}$ ): atmospheric fluxes to soils (northern Spain). *Environ. Sci. Technol.* 41 (4), 1324–1330.
- Sanders, C.J., Santos, I.R., Silva-Filho, E.V., Patchineelam, S.R., 2006. Mercury flux to estuarine sediments, derived from  $^{210}\text{Pb}$  and  $^{137}\text{Cs}$  geochronologies (Guaratuba Bay, Brazil). *Mar. Pollut. Bull.* 52 (9), 1085–1089.
- Schettler, G., Mingram, J., Negendank, J.F., Jiaqi, L., 2006. Palaeovariations in the East-Asian monsoon regime geochemically recorded in varved sediments of Lake Sihailongwan (Northeast China, Jilin Province). Part 2: a 200-year record of atmospheric lead- $^{210}\text{Pb}$  flux variations and its palaeoclimatic implications. *J. Paleolimnol.* 35 (2), 271–288.
- Spalding, Kirsty L., et al., 2005. Forensics: age written in teeth by nuclear tests. *Nature* 437.7057, 333–334.
- Turekian, K.Y., Nozaki, Y., Benninger, L.K., 1977. Geochemistry of atmospheric radon and radon products. *Annu. Rev. Earth Planet. Sci.* 5, 227.
- Van Beek, P., Souhaut, M., Lansard, B., Bourquin, M., Reyss, J.-L., Von Ballmoos, P., Jean, P., 2013. LAFARA: a new underground laboratory in the French Pyrenees for ultra low-level gamma-ray spectrometry. *J. Environ. Radioact.* 116, 152–158.
- Vanneste, H., De Vleeschouwer, F., Bertrand, S., Martínez-Cortizas, A., Vanderstraeten, A., Mattielli, N., Coronato, A., Piotrowska, N., Jeandel, C., Roux, G.L., 2016. Elevated dust deposition in Tierra del Fuego (Chile) resulting from Neoglacial Darwin Cordillera glacier fluctuations. *J. Quat. Sci.* 31 (7), 713–722.